Walisongo Journal of Chemistry
Walisongo Journal of Chemistry Vol. 8 Issue 1 (2025), 12-23
ISSN: 2621-5985 (online); 2549-385X (print)
DOI: https://doi.org/10.21580/wjc.v8i1.22632

THE KINETICS AND OXIDATION OF NEUTRAL RED BY ClO_3^- IN AN AQUEOUS ACIDIC MEDIUM

Patricia Ese Umoru[1*], Ikeckuwku Ugbaga Nkole[2], Joyce Felicity Micheal[1]

[1]Department of Chemistry, Faculty of Science, Nigerian Defence Academy, Kaduna, Nigeria
[2]Basic Science Unit, College of Science & Computing, Wigwe University, Isiokpo, Nigeria

*Corresponding author: peumoru@nda.edu.ng

Abstract

The kinetics and oxidation of neutral red by chlorate ion were studied in an aqueous hydrochloric acid medium at 300 K, with an ionic strength (μ) of 0.2 M (NaCl), by monitoring the absorbance of neutral red (NR) at 515 nm. The reaction was found to be first order concerning both [NR] and [ClO_3^-], with a stoichiometric mole ratio of 1:1 between NR and ClO_3^-. The effect of ionic strength variations was further confirmed by observations that the reaction rate was independent of changes in ionic strength and that the addition of cations had no effect on the rate. No evidence of active radical involvement was observed. The experimental rate law determined was: Rate = ($Kk_3[H^+]$)[NR][ClO_3^-]. Based on the experimental results, an outer-sphere mechanistic pathway is proposed.

Keywords: *Acidic Medium, Chlorate Ion, Kinetics, Neutral Red, Oxidation.*

Introduction

The chlorate ion (ClO_3^-) is an inorganic substance with a strong oxidizing capacity (Jeffrey, 2019) and can be used in the preparation of homemade explosives (Cajigas et al., 2019; Yeager, 2011). Levanov et al. (2008) described the formation of chlorate as the main product of the thermal (non-photochemical) reaction between ozone and chloride ion in alkaline solutions at pH 8.4–10.8 and measured the rate of this process. Chlorate ions have also been reported in water processing applications (Hou et al., 2018; Wang et al., 2015). Structurally, the chlorate ion is trigonal pyramidal. It is utilized in the manufacture of inks, pesticides, textiles, leather, paper goods, and pharmaceuticals (Francois & Josee, 2019). Chlorate ion (ClO_3^-) is formed as a by-product during the disinfection of drinking water, food production water, and the sanitization of food contact surfaces on equipment, especially when chlorine, chlorine dioxide, or hypochlorite is employed (EFSA, 2015). Additionally, at high temperatures, the breakdown of chlorate produces oxygen (Greenwood & Earnshaw, 1997). Chlorates, combined with hydrochloric acid, can also be used to chlorinate aromatic compounds without the need for organic solvents (Sharma, 2014). Furthermore, chlorates are effective in controlling weeds such as Morning Glory, Canada Thistle, Johnson Grass, and St. John's Wort (OHR, 1995; USEPA, 1994). Primarily, as reported by Youngblut et al. (2016), chlorate is employed as a herbicide to treat specific areas and eradicate plants along roadsides, ditches, fences, and other similar

areas. Research has also demonstrated that these herbicides are effective in defoliating and stripping the leaves of various crops, including rice, sunflowers, southern peas, sorghum, cotton, corn, flax, peppers, and soybeans (Kidd & James, 1991; USEPA, 1994).

Neutral Red (NR) is a eurhodin dye widely used for staining living cells and was first demonstrated to serve as a CO_2 sensor due to its unique optical properties, which change with dissolved carbon dioxide (dCO_2) concentrations (Erison et al., 2021). Neutral Red has a variety of applications in biological systems (Repetto et al., 2008; Victor, 2022). It is also used in the dyeing of silk, paper, and cotton, as well as in the production of inks (Ibrahim et al., 2016; Salem, 2002). In an eco-toxicological safety report by Kastury et al. (2015) and at http://www.tiem.utk.edu/~gross/bioed/webmodules/phbuffers.html, acute toxicity values for NR were observed to lie between 2.5×10^{-4} M and 0.01 M.

Despite these uses, the direct assessment of the redox activities of Neutral Red with the strong oxidizing agent chlorate has not been reported. Hence, there is a high possibility that chlorate could affect the chemistry of Neutral Red, given its applications in pharmaceuticals, pesticides, inks, leather, and as a bleaching agent. The work by Levanov et al. (2008), cited in Levanov et al. (2019), remains a preliminary investigation, as basic kinetic parameters such as reaction order, temperature effects, and ionic strength were not explored. Furthermore, the scarcity of research on the kinetics and mechanism of the reaction between Neutral Red and chlorate ions has prompted the authors to undertake this study. Therefore, this research offers deeper insight into the reaction pathways of Neutral Red and chlorate ions. Additionally, the kinetic data generated and the proposed mechanisms will contribute to the conceptual understanding of the redox mechanisms of dyes.

Methodology

Materials

Distilled water was used to prepare stock solutions for all experiments. Analytical-grade reagents were employed throughout the study without any additional purification. The following materials were obtained from Merck: distilled water, glassware, thermometer, UV-visible spectrophotometer (Model 721, PEC Medical), neutral red, sodium chlorate, sodium chloride, sodium nitrate, sodium carbonate, methyl orange, and silver nitrate. Hydrochloric acid, acrylamide, methanol, and diethyl ether were sourced from BDH, Nigeria.

Investigation procedure

The stoichiometry of the reaction was determined using the mole ratio method in spectrophotometric titration (Khan, 2016; Umoru & Effiong, 2022a). The oxidant concentration varied from 1:0.2 to 1:2 (oxidant/reductant), while the dye concentration remained constant. The conditions for the NR/ClO_3^- system were as follows: D = 80.1, [ClO_3^-] = (4.0–40.0) × 10^{-5} M, λ_{max} = 515 nm, [NR] = 2.0 × 10^{-5} M, μ = 0.2 M (NaCl), and T = 300 K. A few drops of dilute nitric acid and silver nitrate solution were added dropwise to the already oxidized mixture. Additionally, a glowing wooden splint was introduced into the mixture to test for oxidation products (Vogel, 2000).

A UV-visible spectrophotometer (Model 721, PEC Medical) was used to measure the absorbance of the fully reacted solutions (A∞) at 515 nm after approximately thirteen hours. The acquired absorbances were plotted against the mole ratios of the reactants. The point of inflection in the plot indicated the reaction's stoichiometry.

The reaction rate between the oxidant and neutral red was studied by monitoring the decrease in absorbance of the dye at its λ_{max} using the same UV-visible spectrophotometer. For all kinetic measurements, [ClO_3^-] was at least 200 times greater than [NR] at the experimental

temperature, ensuring pseudo-first-order conditions. The ionic strength and $[H^+]$ of the reaction medium were kept constant (Ibrahim et al., 2016).

Pseudo-first-order plots were constructed using the linear least squares method, plotting log (At - A∞) versus time (s). The pseudo-first-order rate constants (k_1) were obtained from the slopes of these plots. The second-order rate constants (k_2) were then calculated using $k_2 = k_1/[ClO_3^-]$. The slope of the plot of log k_1 versus log [NR] revealed the reaction order with respect to the oxidant (Ibrahim et al., 2016; Nkole et al., 2023; Umoru & Effiong, 2022b).

At constant ClO_3^- and NR concentrations, as well as constant ionic strength and temperature, the effect of $[H^+]$ on the reaction rate was examined by varying $[H^+]$. A plot of log k_1 versus log $[H^+]$ provided the order of the reaction with respect to hydrogen ion concentration (Nkole et al., 2022b).

The ionic strength of the reaction mixture was varied while maintaining constant ClO_3^-, NR, and $[H^+]$ concentrations at 300 K. The relationship between the reaction rate and changes in ionic strength was determined by plotting log k_2 versus $\sqrt{\mu}$, yielding a slope of 1.02ZAZB. The reactants' charges at the activated complex are represented by ZA and ZB, as shown in Equation 1 (Nkole et al., 2021):

$$\text{Log } k = \log ko + 1.02Z_AZ_B\sqrt{\mu} \quad (1)$$

The effect of the dielectric constant of the reaction medium on the reaction rate was investigated by varying the quantities of acetone in the reaction mixtures while keeping other conditions constant. A plot of log k_2 versus D^{-1} (where D is the dielectric constant) was used to analyze this relationship (Osunkwo et al., 2018). The dielectric constant was calculated using Equation 2 as follows.

$$D_{mixture} = \frac{(V(cm^3) \text{ of ethanol} \times D \text{ of ethanol}) + (V(cm^3) \text{ of water} \times D \text{ of water})}{\text{Total volume of solution}} \quad (2)$$

Notes:
V = volume

The effect of added ions on the reaction rate was studied by introducing different concentrations of NO_3^- and Mg^{2+} ions while keeping the concentrations of ClO_3^-, NR, and HCl constant, along with constant temperature and ionic strength. Additionally, the generation of free radicals in the reaction medium was tested by adding 0.5 cm^3 of 0.1 M acrylamide solution to a partially oxidized reaction mixture containing ClO_3^- and NR. Control experiments were conducted by independently adding acrylamide solution with excess methanol to ClO_3^- and NR solutions (Nkole et al., 2022b).

Finally, kinetic and spectroscopic techniques were employed to check for the presence of a stable, identifiable intermediate species during the reaction. The spectroscopic method involved recording the electronic spectra of partially reacted mixtures at intervals between 400 and 800 nm. The kinetic method involved constructing a Michaelis–Menten plot of $1/k_1$ versus $1/[ClO_3^-]$ (Umoru & Babatunde, 2019).

Results and Discussion

Stoichiometric and Product Analysis

The stoichiometric investigation of the oxidation of neutral red by chlorate ion revealed that one mole of dye was consumed by one mole of ClO_3^-. In contrast, the oxidation of Orange II dye by chlorate ion exhibited a different mole ratio of 1:2 (OR: ClO_3^-) (Myek et al., 2020). The oxidation process produced an organic product, oxygen gas, and chloride ion as a result of the reactants' molar contributions. Figure 1 displays the titration curve, while Equation 3.0 presents the stoichiometric equation for the reaction. The presence of chloride ions was confirmed by the formation of a curdy white precipitate upon the addition of silver nitrate to the ether layer of the product mixture. Oxygen gas generation was validated by the re-ignition of a glowing splint upon exposure to the heated product mixture (Vogel, 2000). The products formed at the end of the reaction are shown in Equation 3 as follows:

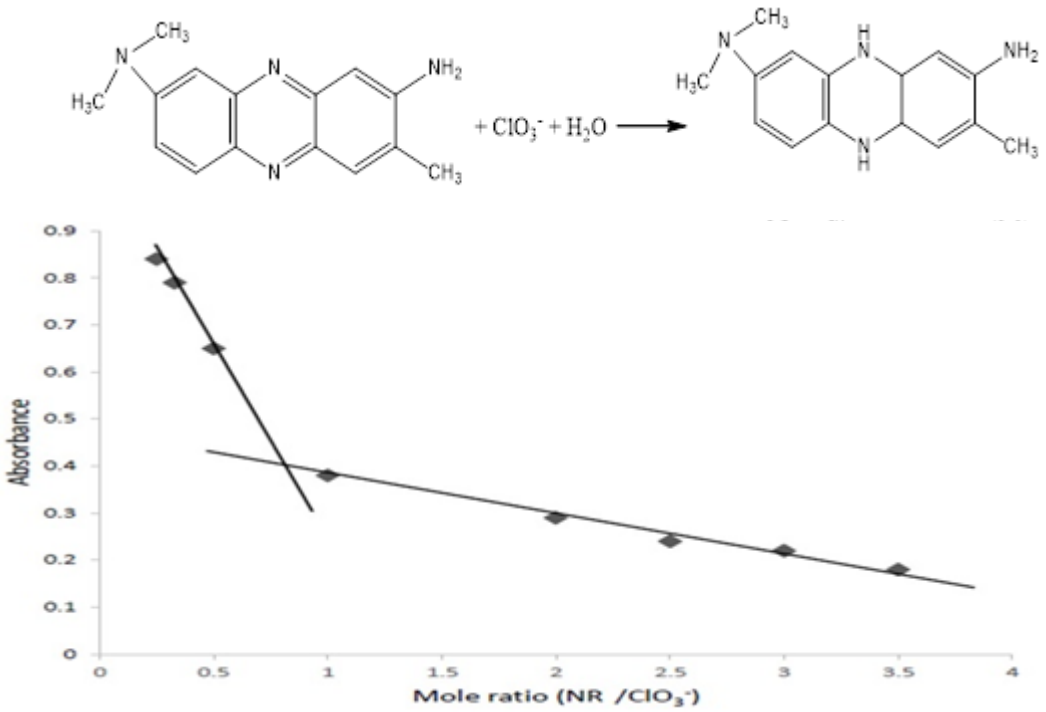

Figure 1. Plot of absorbance versus mole ratio for the determination of the stoichiometry of the oxidation of NR with ClO_3^- at [NR] = 2.0 × 10^{-5} M, [H^+] = 3.0 × 10^{-3} M, μ = 0.2 M, and T = 300 K.

Determination of Pseudo-First-Order, Second-Order Rate Constants, and Order of Reaction

The reaction appeared to be first-order concerning [NR], based on the linear plots of log (A_t – A_∞) versus time, where A_t and A_∞ were the absorbance values at time t and reaction completion, respectively, under pseudo-first-order conditions. Pseudo-first-order rate constants (k_1) were determined from these plots.

A typical plot is shown in Figure 2. The slope of the plot of log k_1 against log [ClO_3^-] (see Figure 3) produced an R^2 value of 1, indicating that the reaction was first-order concerning [ClO_3^-]. As presented in Table 1, the second-order rate constants (k_2) derived from k_1/[ClO_3^-] were relatively consistent. The rate law for the reaction can thus be expressed in Equation 4 as follows.

$$\frac{-d[NR]}{dt} = k_2[NR]ClO_3^-] \quad (4)$$

Effect of Hydrogen Ion Concentration on the Reaction Rate

Protonation of ClO_3^- ions during the reaction (Equation 6.0) caused an increase in the reaction rate with increasing [H^+] (see Table 1). This finding contrasts with Hassan et al. (2021), who observed a decrease in rate with increasing [H^+]. A direct acid dependency plot of log k_1 versus log [H^+] (see Figure 4) produced a straight line with a slope of 0.763, indicating a positive dependency. The overall rate equation based on this observation is depicted in Equation 5.

$$\frac{-d[NR]}{dt} = (a[H^+])[NR][ClO_3^-] \quad (5)$$

Notes:
a is the slope representing the reaction's acid dependency.

Table 1. Pseudo-first-order and second-order rate constants for the oxidation of NR with ClO_3^- at [NR] = 2.0 × 10^{-5} M, T = 300 K, and λ_{max} = 515 nm.

10^3 [ClO_3^-], M	10^3 [H^+] M	μ, M	$10^3 k_1$, s^{-1}	k_2 M s^{-1}
4.00	3.00	0.20	8.08	2.02
5.00	3.00	0.20	10.15	2.03
6.00	3.00	0.20	12.18	2.03
7.00	3.00	0.20	14.14	2.02
7.50	3.00	0.20	15.30	2.04
8.00	3.00	0.20	16.15	2.02
8.50	3.00	0.20	17.25	2.03
9.00	3.00	0.20	18.27	2.03
7.00	1.00	0.20	7.01	0.87
7.00	2.00	0.20	10.34	1.56
7.00	3.00	0.20	14.14	2.03
7.00	4.00	0.20	18.76	2.61
7.00	5.00	0.20	22.23	3.07
7.00	6.00	0.20	26.98	3.45
7.00	7.00	0.20	30.21	3.89
7.00	8.00	0.20	34.42	4.24
7.00	3.00	0.05	14.13	2.02
7.00	3.00	0.08	14.14	2.03
7.00	3.00	0.10	14.12	2.03
7.00	3.00	0.15	14.12	2.03
7.00	3.00	0.20	14.13	2.03
7.00	3.00	0.25	14.13	2.04
7.00	3.00	0.30	14.13	2.04
7.00	3.00	0.40	14.14	2.04

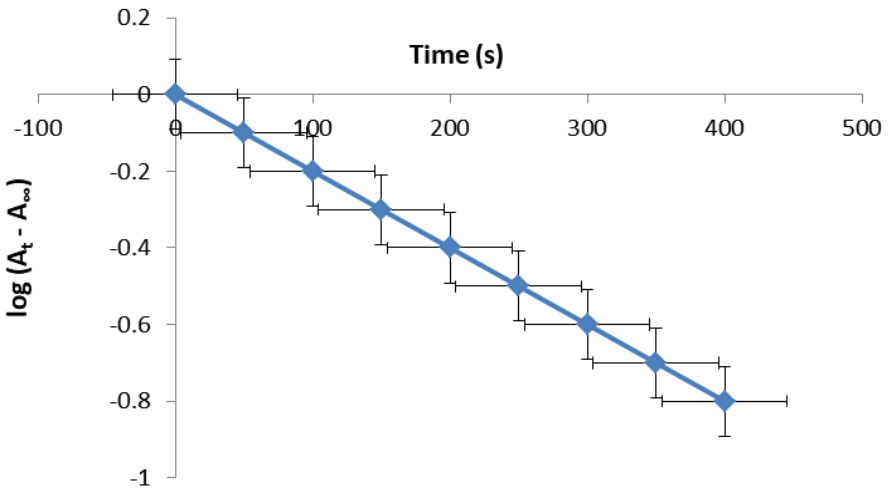

Figure 2. Typical pseudo-first-order plot for the oxidation of NR with ClO_3^- at [NR+] = 2.0×10-5 M, [ClO_3^-] = 7.0 × 10-3M, [H+] = 3.0 × 10-3 M, μ = 0.20 M, λmax = 515 nm, and T = 300 K.

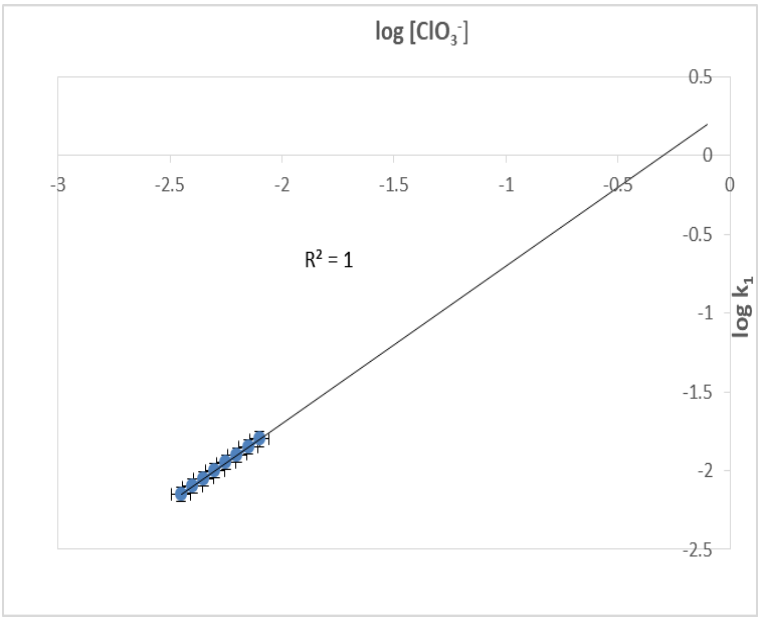

Figure 4. Plot of log k1 versus log [ClO_3^-] for the oxidation of NR with ClO_3^- at [NR] = 2.0 × 10-5 M, [ClO_3^-] = 7.0 × 10^{-3} M, [H+] = 3.0 × 10-3 M, μ = 0.20 M, T = 300 K, and λmax = 515 nm.

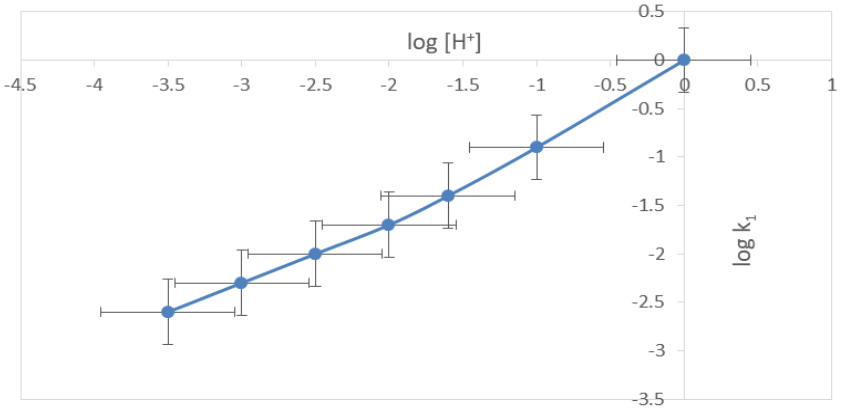

Figure 3. Plot of log k1 versus log [H^+] for the oxidation of NR with ClO_3^- at [NR] = 2.0 ×10-5 M, [ClO_3^-] = 7.0 × 10^{-3} M, μ = 0.20 M, and T = 300 K

Effect of Ionic Strength and Dielectric Constant on the Reaction Rate

The reaction rate remained unchanged with increasing ionic strength (see Table 1), suggesting that uncharged species interacted at the rate-determining step (Equation 7). Similarly, variations in the dielectric constant (see Table 2) did not affect the reaction rate. These findings contrast with previous studies (Abdulsalam, 2016; Adetoro, 2021; Bugaje, 2021; Ibrahim & Hamza, 2016), which reported a decrease in reaction rate with increasing ionic strength.

Effect of Added Ions on the Reaction Rate

As shown in **Table 3**, the addition of ions (NO_3^- and Mg^{2+}) to the reaction medium did not have a significant effect on the reaction rate, indicating no catalytic or inhibitory effect. This suggests that the reaction involved uncharged species at the rate-determining step. This observation contrasts with that reported by Osunlaja (2012).

Table 2. Effect of changing the dielectric constant on the oxidation of NR with ClO_3^- at [NR] = 2.0 ×10^{-3} M, [ClO_3^-] = 7.0 × 10^{-3} M, [H^+] = 3.0 × 10^{-3} M, μ = 0.20 M, T = 300 K, and λ_{max} = 515 nm.

D	10^2 1/D	k_1, s^{-1}	k_2, M s^{-1}
80.10	1.24	4.07	2.03
79.72	1.25	4.07	2.03
79.34	1.26	4.05	2.02
78.58	1.27	4.05	2.02
77.44	1.29	4.05	2.02
76.30	1.31	4.03	2.01

Table 3. Effect of added anions and cations on the oxidation of NR with ClO_3^- at [NR] = 2.0 × 10^{-5} M, [ClO_3^-] = 7.0 × 10^{-3} M, [H^+] = 3.0 × 10^{-5} M, μ = 0.20 M, T = 300 K, and λ_{max} =515 nm.

Ion	10^3[Ion], M	k_1, s^{-1}	k_2, M^{-1} s^{-1}
NO_3^-	0.00	4.07	2.03
	10.00	4.58	2.29
	20.00	4.86	2.43
	30.00	5.16	2.59
	40.00	5.18	2.74
	50.00	5.84	2.92
	60.00	6.34	3.17
Mg^{2+}	0.00	4.07	2.03
	10.00	4.05	2.02
	20.00	4.07	2.03
	30.00	4.07	2.03
	40.00	4.05	2.02
	50.00	4.05	2.02
	60.00	4.05	2.02

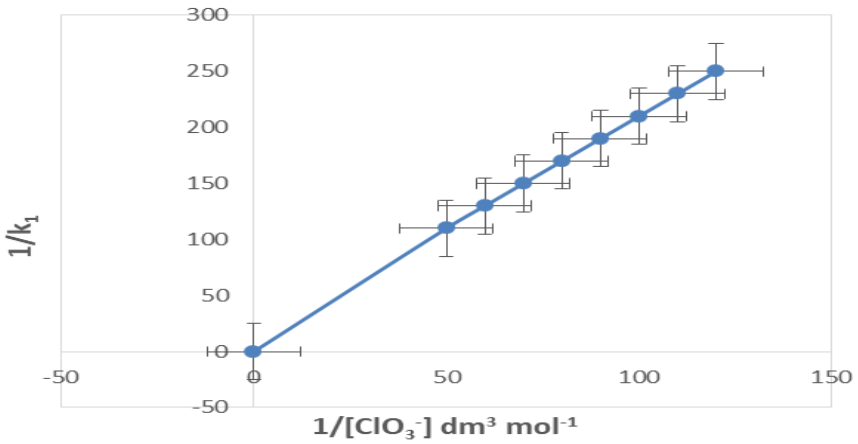

Figure 5. Michaelis-Menten plot of $1/k_1$ versus $1/[ClO_3^-]$ for the oxidation of NR with ClO_3^- at [NR] = 2.0 × 10^{-3} M, $[ClO_3^-]$ = 7.0 ×10^{-3} M, $[H^+]$ = 3.0 × 10^{-3} M, μ = 0.20 M, T = 300 K, and λ_{max} =515 nm.

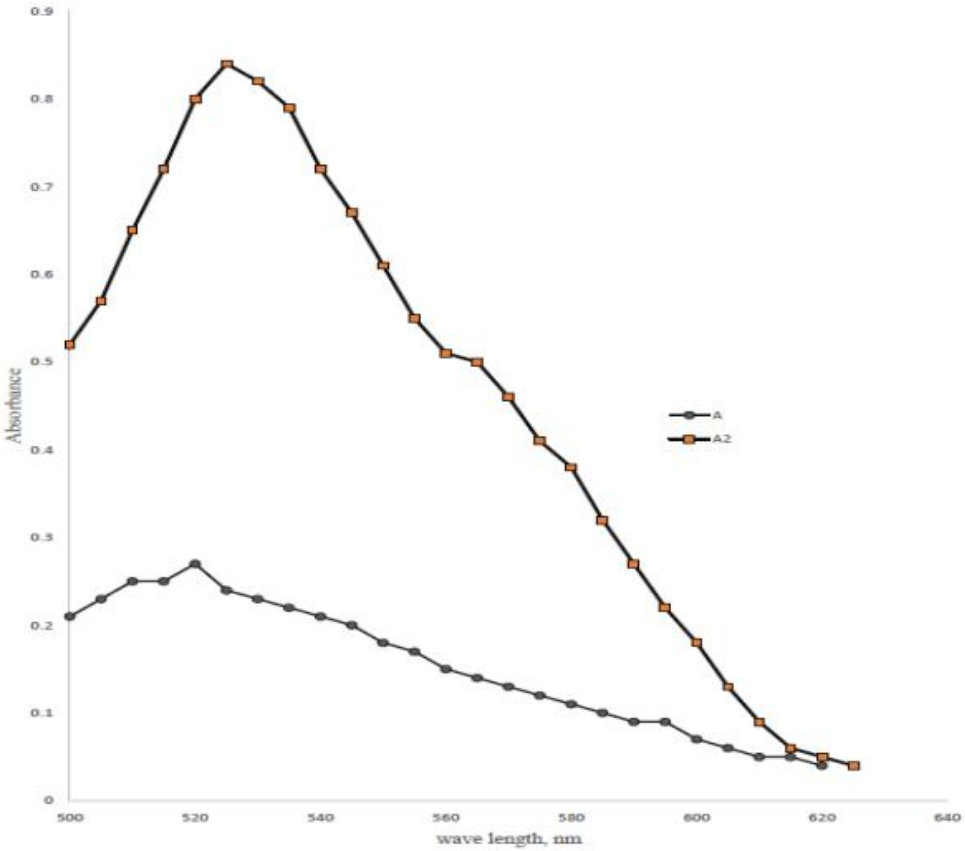

Figure 6. Spectrum of neutral red and the NR–ClO_3^- reaction mixture.

Free Radical Test

The partially reacted mixture of NR and ClO_3^- with excess methanol did not form a gel upon the addition of acrylamide, indicating the absence of free radicals. This finding contrasts with Fawzy (2016), who reported free radical participation during permanganate oxidation of fluorenone hydrazone.

Test for Intermediate Formation

Kinetic Method

The Michaelis-Menten plot of $1/k_1$ versus $1/[ClO_3^-]$ (see **Figure 5**) exhibited a negligible intercept, suggesting that no significant intermediate formation occurred.

Spectroscopic method

The reaction proceeded without the formation of an intermediate complex, as evidenced by the absence of a discernible shift in λ_{max} (515 nm) when the reaction mixture of NR and ClO_3^- was scanned between 400 and 800 nm (see Figure 6).

Based on the following observations, it was highly likely that neutral red was oxidized by ClO_3^- in acidic aqueous media via an outer-sphere mechanism:

I. The negligible intercept on the Michaelis-Menten plot.
II. The absence of complex intermediate formation.The reaction mechanism can be summarized as follows:

$$ClO_3^- + H^+ \rightleftharpoons HClO_3 \quad (6)$$

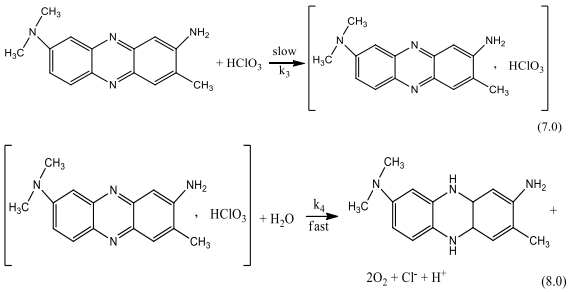

$$Rate = k_3[NR][HClO_3] \quad (9)$$

From Equation 6.0;

$$[HClO_3^-]=K[ClO_3^-][H^+] \quad (10)$$

Substituting Equation 10 into Equation 9;

$$Rate=Kk_3[H^+][NR][ClO_3^-] \quad (11)$$

$$Rate=k[NR][ClO_3^-] \quad (12)$$

where $k = Kk_3[H^+]$ and Equation 12 conforms to Equation 4.

Conclusion

The oxidation mechanism of neutral red in acidic aqueous solution in the presence of chlorate ions has been extensively studied. Irrespective of the concentrations of the oxidant and reductant, the reaction consistently exhibits first-order consumption of the reductant relative to each mole of oxidant produced. Kinetic analysis reveals that the reaction rate constant is highly dependent on the acidity of the solution, highlighting the acid-sensitive nature of the dye's redox behavior. Based on spectroscopic and kinetic data, the reaction is best described by an outer-sphere electron transfer mechanism.

References

Abdulsalam S. & Idris S.O, (2016). Kinetics and Mechanism of Redox Reaction of Crystal Violet and metabisulphite Ion in Aqueous Acidic Medium. Gashua Journal of Sciences and Humanities. 2(2), 19-26.

Adetoro, A, Idris S. O , Onu, A. D & Okibe F. G (2021). Kinetics And Mechanistics

Steps To The Electron Transfer Reaction of Peroxo-Bridged Binuclear Cobalt(III) Complex of Succinimide By Glycine In Aqueous Acidic Medium. Bull. Chem. Soc. Ethiop. 35(2), 425-434

Bugaje, B. M., Idris S. O., Onu, A D. & Shallangwa, G. A. (2021) Kinetics And Mechanism of Oxidation Of Safranin – O By Permanganate Ion In Acidic Medium. Nigerian Research Journal of Chemical Sciences 9(2): 47-62.

Crespo Cajigas, J. M., Perez-Almodovar, L., & DeGreeff, L. E. (2019). Headspace analysis of potassium chlorate using on-fiber SPME derivatization coupled with GC/MS. Talanta, 205, 120127. https://doi.org/10.1016/j.talanta.2019.120127.

EFSA panel on contaminants in the food chain. (2015) Risks for public health related to the presence of chlorate in food. EFSA Journal 13, 4135.

Ericson, M. N, Shankar, S. K., Chahine, L. M., Omary, M. A., Herbing, L. H. V. &. Marpu, S. B. (2021). Development of Neutral Red as a pH/pCO2 Luminescent Sensor for Biological Systems Chemosensors 9(8), 210; https://doi.org/10.3390/chemosensors9080210

Fawzy, A., Ahmed, S. A., Althagafi, I. I., Morad, M. H.& Khariou K. S., (2016). Kinetics and Mechanistic Study of Permanganate Oxidation of Fluorenone Hydrazone in Alkaline Medium. Advances in Physical Chemistry https://doi.org/10.1155/2016/4526578

Francois, M. & Josee, B., (2019). Plasmapheresis in acute intoxication and poisoning. Medicinal Journal of Francois, Critical care nephrology (3rd edition) 595 - 600,

Greenwood, N. & Earnshaw, A. (1997). Chemistry of the Elements (2nd ed.). Butterworth-Heinemann. ISBN 978-0-08-037941-8.

Hassan, M, Al-Hakimi A.N. & Alahmadi, M.D. (2001). Kinetics of Oxidation of Aliphatic Alcohols by Potassium Dichromate in Aqueous and Micellar Media S. Afr. J. Chem., 64: 237–240.

Hou, S et al., (2018). Chlorate formation mechanism in the presence of sulfate radical, chloride, bromide and natural organic matter Environ. Sci. Technol.

Ibrahim I., Idris S.O. & Onu, A.D. (2016). Kinetics and mechanism of redox reaction of neutral red with nitrite ion in aqueous acidic medium. International Letters of Chemistry, Physics and Astronomy, 67: 50-57.

Ibrahim, I. and Hamza, S. A. (2016). Kinetics and mechanism of redox reaction of neutral red and bromate ion in aqueous acidic medium. FUW Trends in Science and Technology Journal, 1(1): 216- 220.

Ibrahim, I., Idris, S.O., Abdulkadir, I. & Onu, A. D. (2018). Kinetics and mechanism of the redox reaction of n,n′-phenylenebis-(salicylideneiminato)iron(III) with oxalic acid in mixed aqueous medium. Transition Metal Chemistry, 44(3), 269–273.

Jeffery, G.H., Bassett, J. Mendham, J. & Denney, R. C. (2000). Vogel's Textbook of Quantitative Chemical Analysis (6th edition), 214-216; 312-315.

Kastury, F.; Juhaszb, A.; Beckmanna, S. & Manefield, M. (2015). Ecotoxicity of neutral red (dye) and its environmental applications. Ecotoxicol. Environ. Saf. 122, 186–192. [Google Scholar] [CrossRef]

Kaushik, M., & Jeffrey, G.C. (2019) Chlorate as a potential oxidant on mars: rates and products of dissolved Fe (II) oxidation. Journal of Geophysical Research, 124(11), 2893 - 2916.

Khan, S. R., Ashfaq M. & Summyia M. (2016). Oxidation Kinetics of Crystal Violet by Potassium Permanganate in Acidic Medium 1 Russian Journal of Physical Chemistry 90(90 00000):955-96 DOI: 10.1134/S0036024416050265.

Levanov, A.V., Kuskov, I.V., Antipenko, E.E., & Lunin, V.V., 2008. The solubility of ozone and kinetics of its chemical

reactions in aqueous solutions of sodium chloride. Russ. J. Phys. Chem. 82, 2045e2050. https://doi.org/10.1134/ s0036024408120133

Levanov, A. V., Isaikina, O.Y. , Gasanova , R. B., Uzhel, A. S. &. Lunin, V. V. (2019). Kinetics of chlorate formation during ozonation of aqueous chloride solutions. Chemosphere, 229: 68-76.

Myek, B., Idris, S.O., Onu, A.D. & Yakubu, M.K. (2020). Kinetics and mechanism of the oxidation of orange ii by chlorate ion in aqueous hydrochloric acid. Communication in Physical Sciences, 5(2), 165-170.

Nkole, I.U. & Idris, S.O. (2021). Thermodynamics and kinetic investigation of reaction of acriflavine with l-cysteine in aqueous medium. Chemistry Africa,4: 731 – 740

Nkole, I.U., Idris, S.O., Abdulkadir, I. & Onu, A.D. (2022b). The study of redox reaction of gallic acid with bis-(2-pyridinealdoximato)dioxomolybdate(IV) complex in an aqueous acidic medium. Chemistry Africa, https://doi.org/10.1007/s42250-022-00346-z

Nkole, I.U., Idris, S.O., Abdulkadir, I. & Onu, A.D. (2023). Cationic surfactant-based catalysis on the oxidation of glutamic acid by bis-(2-pyridinealdoximato)dioxomolydate(IV) complex. Catalysis Letters, https://doi.org/10.1007/s10562-022-04187-w.

OHS Database. February, 1995. MSDS for Acetochlor. MDL Information Systems Inc., San Leandro, CA.

Osunkwo, C. .R., Nkole, I.U., Onu, A.D. & Idris, S.O. (2018). Electron transfer reaction of tris(1,10-phenanthroline)cobalt (III) complex [co(phen)3]3+ and thiosulphate ion (S2O32−) in an aqueous acidic medium.International Journal of Advance Chemistry, 6: 121 - 126.

Osunlaja, A. A., Idris, S. O. & Iyun, J.F., (2012). Kinetics and Mechanism of the Methylene Blue– Permanganate ion Reaction in Acidic Medium. Archi Applied Science Research, 4(2), 772 – 780

Patnaik, S. K. Maharana, P. K. Saku, S. N. & Murty, G.S.N. (1991). Solid phase oxidation of iodide ion by bromate, chlorate and perchlorate and the role of gamma radiation. Journal of Radioanalytical and Nuclear Chemistry, 152, 1261- 271.

Repetto G, del Peso A & Zurita J. L (2008). Neutral red uptake assay for the estimation of cell viability/cytotoxicity. Nat. Protoc., 3: 1125–1131

Salem I. A., (2002). Kinetics and mechanisms of the non- catalyzed and manganese(II) catalyzed oxidation of neutral red with potassium periodate in aqueous solution. Zeitschrift für physikalische Chemie., 216, 991-1003.

Sharma, SK & Agarwal, D. D. (2014). "Oxidative Chlorination of Aromatic Compounds in Aqueous Media" (PDF). International Journal of Scientific and Research Publications, 4 (7).

The University of Tennessee, Knoxville; The Institute of Environmental Modeling. Alternative Routes to Quantitative Literacy for the Life Sciences. Maintaining Cellular Conditions: pH and Buffers. Available online: http://www.tiem.utk.edu/~gross/bioed/webmodules/phbuffers.html (accessed on 17 July 2019).

Umoru, P.E. & Babatunde, O.A. (2019). Kinetics and mechanism of the oxidation of sulphite ion by di-μ-oxo-tetrakis(2,2'-bipyridine)-dimanganese(III, IV) perchlorate in aqueous acidic medium. Journal of Chemical Society of Nigeria, 44(4): 710 – 717.

Umoru, P.E. & Effiong, U.I. (2022a). Kinetics and oxidation of the reactions between dithionite ion and nitrocellulose in acidic phase. FUDMA Journal of Sciences, 6(2), 221 – 226.

Umoru, P.E. & Effiong, U.I. (2022b). Kinetics and mechanism of the reduction of tartrazine by nitrite ion in aqueous

acid phase. Academic Journal of Chemistry, 7(1), 10 –16.

USEPA (U.S. Environmental Protection Agency) 1994. Pesticide Tolerances or Acetochlor. Federal Register. 59, No. 56. Rules and Regulations. 23

Victor, V.K., (2022). Excitation of neutral red dye in aqueous media: comparative theoretical analysis of neutral and cationic form. Journal of Molecular Modelling, 28(4), 130 – 140.

Villata, L.S., Martire, D.O., & Capparelli, A. L. (1995). Oxidation of bromide by chlorate ion Journal of Molecular Catalysis, 99(3), 143- 149.

Wang D. et al., (2015) Formation of disinfection by-products in the ultraviolet/chlorine advanced oxidation process Sci. Total Environ.

Youngblut M. D., Wang O., Barnum T.P., Coates J. D. (2016). (Per)chlorate in biology on earth and beyond. Annu. Rev. Microbiol. 70:435–457. doi: 10.1146/annurev-micro-102215-095406. [DOI] [PubMed] [Google Scholar]